VNU Journal of Science: Mathematics – Physics, Vol. 32, No. 2 (2016) 34-42

Characterizing Stochastic Errors of MEMS – Based Inertial Sensors

Pham Van Tang[1,*], Tran Duc Tan[2], Chu Duc Trinh[2]

[1]*Military Academy of Logistics, Hanoi, Vietnam*
[2]*VNU University of Engineering and Technology, 144 Xuan Thuy, Hanoi, Vietnam*

Received 14 April 2016
Revised 15 May 2016; Accepted 24 June 2016

Abstract: Thank to strong grow of MicroElectroMechanicalSystem (MEMS) technology, high performance and small size sensors are widely used in many areas such as landslide, navigation, mobile phones, etc. However, there are several kinds of errors are still existing in MEMS based sensors that need a carefully analyzing and calibration. By each year, the performances of commercial sensors are also improved. In this paper, we focused on characterizing the stochastic errors of accelerometers and gyroscopes integrated with a latest smart phone of Apple Inc. Iphone6+. The MP67B is a custom version of the InvenSense 6-Axis device (3-Axis gyroscope and 3-Axis accelerometer) made for Apple. This research will play an important step to decide whether we can create an Inertial Navigation System (INS) in the same device (i.e. the smart phone, the users do not need to equip a single device for positioning application). The Allan variance method is exploited to analyze the stochastic errors in these sensors. Experiments proved that the main sources of errors in these sensors are white noises. The Iphone5 can operate as a low-cost solution of positioning and navigation device.

Keywords: Sensor, MEMS, Stochastic Errors.

1. Introduction

Nowadays, thanks to the progress of MEMS technology, the inertial sensor become smaller, cheaper and more precise. They are widely used in the INS/GPS integrated systems. However, the measurement data of sensors are usually affected by different types of error sources, such as sensor noises, scale factor, and bias variations, etc. This sensors need testing and calibration before applying to real applications. Based on different error sources, the errors which exist in inertial sensors can be divided into deterministic errors and stochastic errors [1-3]. Major deterministic error sources include bias, scale errors, which can be removed by specific calibration procedures [1], [4]. The stochastic errors include Quantization Noise, Random Walk, Bias Instability (1/f or flicker noise), Rate Random Walk and Rate Ram [5]. The random errors cannot be removed from the measurements and should be

* Corresponding author. Tel.: 84-983711805
E-mail: phamvantang@gmail.com

reduced by the filters. Therefore, the analysis and the characterization of random errors of MEMS inertial sensors are a necessity to improve the accuracy [6].

The Allan variance (AV) and the Power Spectral Density (PSD) are two main methods used to estimate the stochastic characterization existing in inertial sensors. The PSD is the most commonly used representation of the spectral decomposition of a time series. It is a powerful tool for analyzing and characterizing data, and for stochastic modelling [5]. The Allan variance is a time domain analysis technique originally developed to study the frequency stability of oscillators. This method was initially studied by David Allan in 1966 [7]. The Allan variance is a method of representing the root mean square (RMS) random-drift errors as a function of averaging times. It is simple to compute and relatively simple to interpret and understand. The Allan variance method can be used to determine the characteristics of the underlying random processes that give rise to the data noise. This technique can be used to characterize various types of noise terms in the inertial sensor data [8].

In this paper, we focused on identification of the stochastic errors of accelerometers and gyroscopes in MP67B IMU which is built in Iphone6 and Iphone6Plus. It will play an important decisive whether we can combine this IMU with a navigation algorithm to create an Inertial Navigation System (INS) in the same device.

2. Allan Variance method

Allan variance analysis is commonly and efficiently used to identify and obtain the variances for most of the random errors. Allan variance is based on the method of cluster analysis. Assume that there are N consecutive data points, each having a sample time of t_0. Forming a group of n consecutive data points (with $n < \frac{N}{2}$), each member of the group is a cluster (Fig. 1).

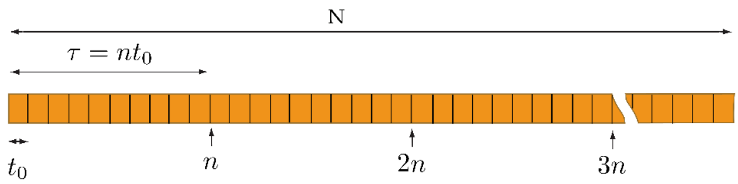

Fig 1. Scheme of data structure used in Allan variance algorithm.

Associated with each cluster is a time τ , which is equal to nt_0. If the instantaneous output rate of the inertial sensor is $\Omega(\tau)$, the cluster average is defined as [9]

$$\bar{\Omega}_k(\tau) = \frac{1}{\tau}\int_{t_k}^{t_k+\tau} \Omega(t)\,dt \tag{1}$$

where $\bar{\Omega}_k(t)$ represents the cluster average of the output rate for a cluster, which starts from the *k-th* data point and contains *n* consecutive data points. The definition of the subsequent cluster average is [9].

$$\bar{\Omega}_{next}(\tau) = \frac{1}{\tau}\int_{t_{k+1}}^{t_{k+1}+\tau} \Omega(t)\,dt \tag{2}$$

where $t_{k+1} = t_k + \tau$

The Allan variance of length τ is defined as follows [9]

$$\sigma^2(\tau)=\frac{1}{2}\left\langle\left(\bar{\Omega}_{next}(\tau)-\bar{\Omega}_k(\tau)\right)^2\right\rangle=\frac{1}{2(N-2n)}\sum_{k=1}^{N-2n}\left[\bar{\Omega}_{next}(\tau)-\bar{\Omega}_k(\tau)\right]^2 \tag{3}$$

where < > is the averaging value over the ensemble of clusters.

Clearly, for any finite number of data points (N), a finite number of clusters with length τ can be formed. Hence, equation (3) represents an estimation of the quantity σ^2 (τ), whose quality of an estimate depends on the number of independent clusters of a fixed length that can be formed. The Allan variance is a measure of the stability of the sensor output. A log-log plot of the square root of the Allan variance $\sigma(\tau)$ versus τ provides a means of identifying and quantifying various noise terms that exist in the inertial sensor data. The cluster sampling can be done in following three ways: Fully Overlapping Allan Variance; Non Overlap Allan Variance and Not Fully Overlapping Allan Variance [10].

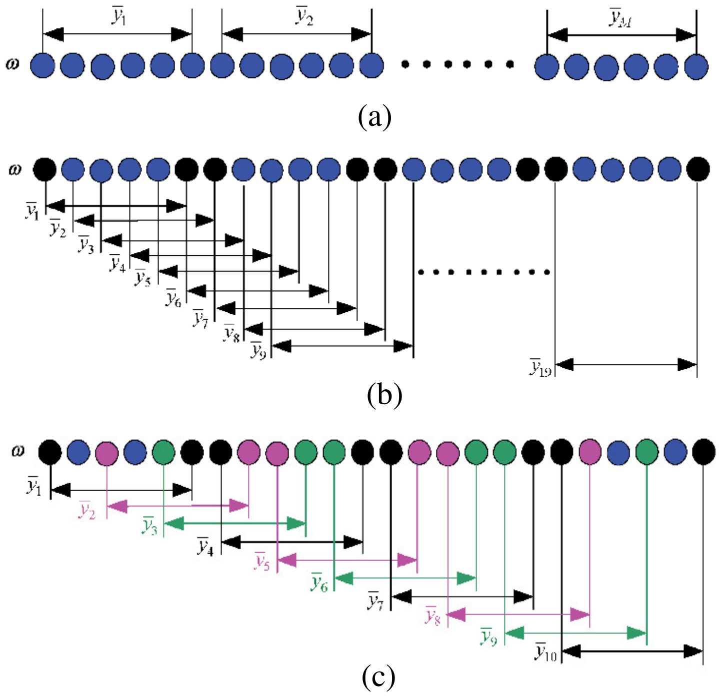

Fig 2. (a) Nonoverlapped cluster sampling method. (b) Fully overlapping cluster sampling method. (c) Not fully over lapping cluster sampling method [10].

3. Analysis of stochastic noise terms in Allan variance

In general, any number of stochastic noise components may be present in the data depending on the type of device and the environment in which the data are obtained. Noise terms in Allan variance, which are known to exist in the inertial sensor data, are represented as given below [5], [11]:

3.1. Quantization noise

This noise is strictly due to the quantized nature of the sensor's output. The quantization noise is inherent in the amplitude quantization process. Allan variance for quantization noise is given by

$$\sigma^2(\tau) = \frac{3Q_z^2}{\tau^2} \tag{4}$$

where Q_z is the quantization noise coefficient and τ is the sample interval. Therefore the quantization noise is represented by a slope of -1 in a log-log plot of $\sigma(\tau)$ versus τ. The magnitude of this noise can be read off the slope line at $\tau = \sqrt{3}$.

3.2. Angle (velocity) random walk

The angle random walk is characterized by a white noise on the gyro angle (or accelerometer velocity) output. The Allan variance for angle (velocity) random walk is given by

$$\sigma^2(\tau) = \frac{Q^2}{\tau} \tag{5}$$

where Q is the angle (velocity) random walk coefficient. Equation (5) indicates that a log-log plot of $\sigma(\tau)$ versus τ has a slope of -1/2. The valued of Q can be obtained directly by reading the slope at $\tau = 1$.

3.3. Bias instability

This noise is also known as flicker noise. The origin of this noise is the electronics, or other components susceptible to random flickering. Because of its low-frequency nature, it shows as the bias fluctuations in the data. Allan variance for bias instability is given by

$$\sigma^2(\tau) = \left(\frac{B}{0.664}\right)^2 \tag{6}$$

Hence, the bias instability value can be read off the root Allan variance plot at the region where the slope is zero.

3.4. Rate random walk

This is a random process of uncertain origin, possibly a limiting case of an exponentially correlated noise with a very long correlation time. The Allan variance of rate random walk is given by

$$\sigma^2(\tau) = \frac{K^2\tau}{3} \tag{7}$$

This indicates that rate random walk is represented by a slope of + 0.5 on a log-log plot of $\sigma(\tau)$ versus τ.

3.5. Rate ramp

This is more of a deterministic error rather than a random noise. It could also be due to a very small acceleration of the platform in the same direction and persisting over a long period of time. Allan variance of rate ramp is given by

$$\sigma^2(\tau) = \frac{R^2\tau^2}{2} \tag{8}$$

This indicates that the rate ramp noise has slope of + 1 in the log-log plot of $\sigma(\tau)$ versus τ.

A typical Allan variance plot is shown in Fig 3. In most cases, different noise terms appear in different regions of τ. This allows easy identification of various random processes that exist in the data. It can be assumed that the Allan variance at any given τ is the sum of Allan variances due to the individual random processes at the same τ

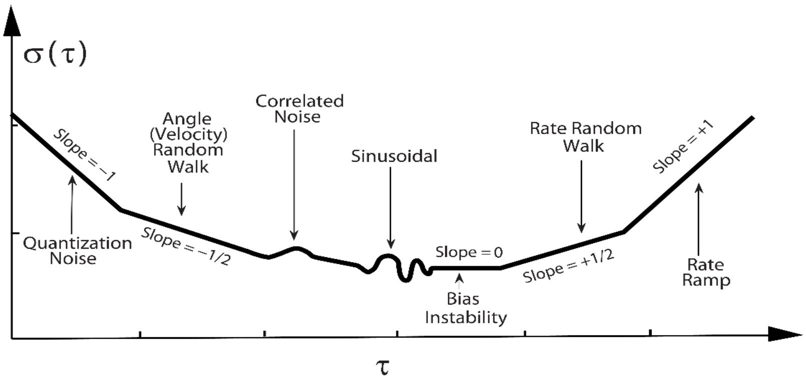

Fig 3. σ(τ) Sample plot of Allan variance analysis results [5].

4. Experiment and result

Figure 4 shows the package views of the MP67B 6-Axis IMU supplied by InvenSense and found in iPhone 6 and 6 Plus. It consists of 3-Axis gyroscope + 3-Axis Accelerometer made for Apple and integrated in the iPhone 6 and iPhone 6 Plus. For the 3-Axis gyroscope, its design now uses a single structure vibratory compared to three different structures for the previous generation of gyros. This new design results in a shrink of 40% of the 3-axis gyro area. The size of the sensor package is 3.0×3.0×0.8 mm^3.

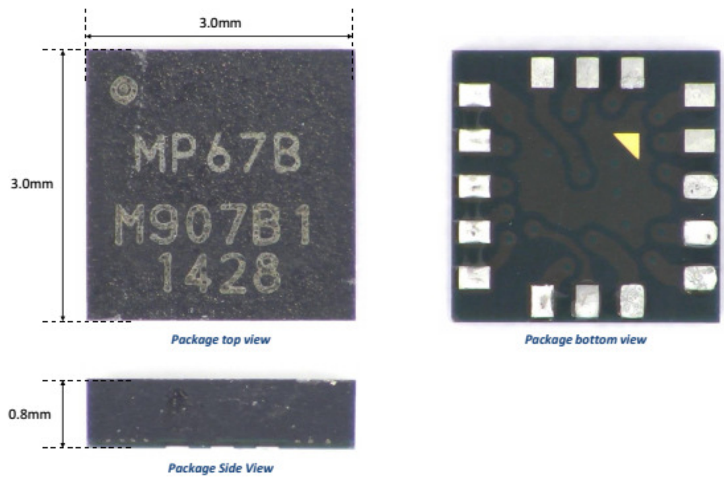

Fig 4. Package views of the MP67B 6-Axis IMU.

Deterministic errors could be eliminated by a careful calibration. Figure 5 shows the photo of this IMU in a calibration process. The sensor data in the first 600 seconds are shown in Fig. 6.

Fig. 5. The device in a calibration process.

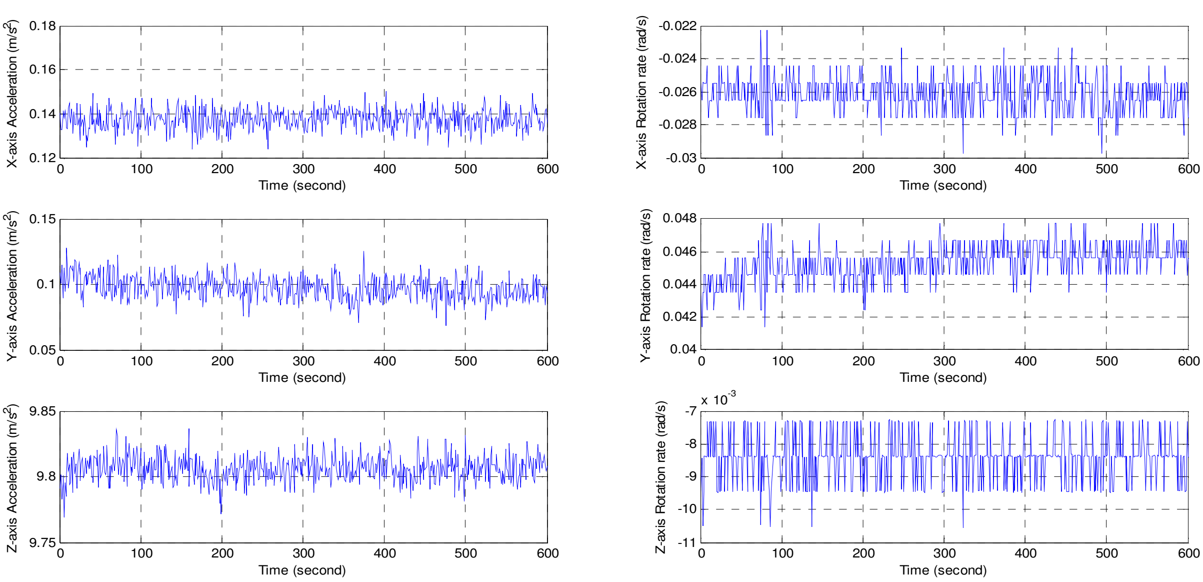

Fig. 6. Sensor data in the first 600 seconds.

In order to characterize the stochastic errors of this IMU, one hour static data was acquired. After that, the Allan method is applied to the whole data set, log-log plot of the Allan standard deviation versus the cluster time is shown in Fig. 7 for the acceleration data and Fig. 8 for the gyro data. Figs. 7 and 8 clearly shown that the random walk is the dominant noise for both the short and long cluster times. For the X-axis acceleration curve, for example, a straight line with a slope of -0.5 fitted to the vertical line of $\tau = 1$ (as mentioned in sub-section 3.2) at a value of 0.0048. Thus, the random walk coefficient for the MP67B X-axis accelerometer is estimated as $Q = 0.0048\dfrac{\frac{m}{s}}{\sqrt{s}} = \dfrac{0.0048\frac{m}{s^2}}{\sqrt{Hz}}$. For the X-axis gyro curve, for example, a straight line with a slope of -0.5 fitted to the vertical line of $\tau = 1$ at a value of 0.0011. Thus, the random walk coefficient for the MP67B X-axis gyro is estimated as $\dfrac{Q = 0.0011\frac{rad}{\sqrt{s}} = 0.0011\frac{rad}{s}}{\sqrt{Hz}}$. Also in Fig. 9, for the long cluster times, the bias instability noise is appeared with its deviation of 0.00026. Thus, the bias instability coefficient is estimated at 0.00039 rad/s.

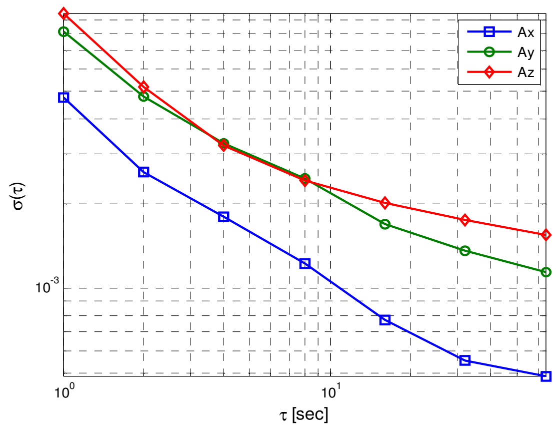

Fig. 7 MP67B accelerometer Allan variance results.

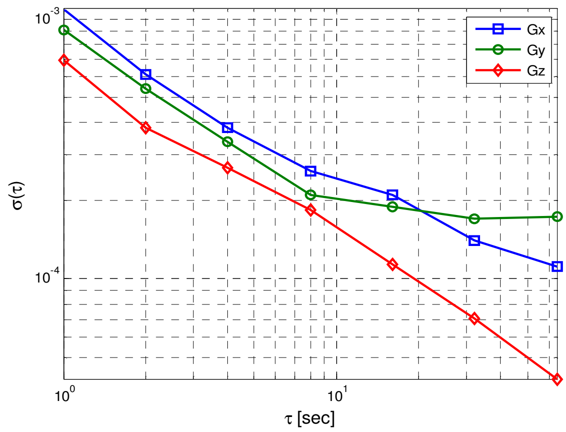

Fig. 8 MP67B gyroscope Allan variance results.

Table 1 lists the identified error coefficients for all of the gyro and acceleration sensors.

Table 1. Identified error coefficient for MP67B

	$Q\left(\frac{\frac{m}{s^2}}{\sqrt{Hz}}\right)$ computed by MDEV	$Q\left(\frac{\frac{m}{s^2}}{\sqrt{Hz}}\right)$ computed by ADEV	Other noises
Ax	0.00480	0.00481	
Ay	0.00820	0.00681	
Az	0.00950	0.01068	
	$Q\left(\frac{\frac{m}{s^2}}{\sqrt{Hz}}\right)$ computed by MDEV	$Q\left(\frac{\frac{m}{s^2}}{\sqrt{Hz}}\right)$ computed by ADEV	
Gx	0.00110	0.00117	
Gy	0.00091	0.00123	Flicker noise: B=0.00039 rad/s.
Gz	0.00069	0.00070	

Power Spectral Density (PSD) shows hơ the power is allotted along the frequency range. For example, Fig. 9 shows a log-log plot of PSD of the X-axis accelerometer. PSD of this data is fitting to S(f) = f^(-0.029). It closes to white noise (i.e. random walk). Fig. 10 shows a log-log plot of PSD of the Y-axis gyro. PSD of this data is fitting to a S(f) = f^(-0.61). The spectrum is close to flicker noise (i.e. bias instability).

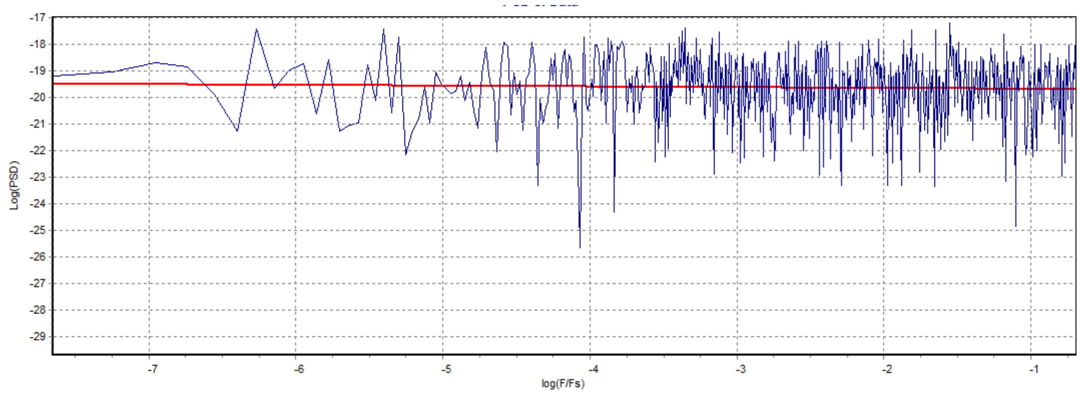

Fig. 9. MP67B X-axis accelerometer PSD result.

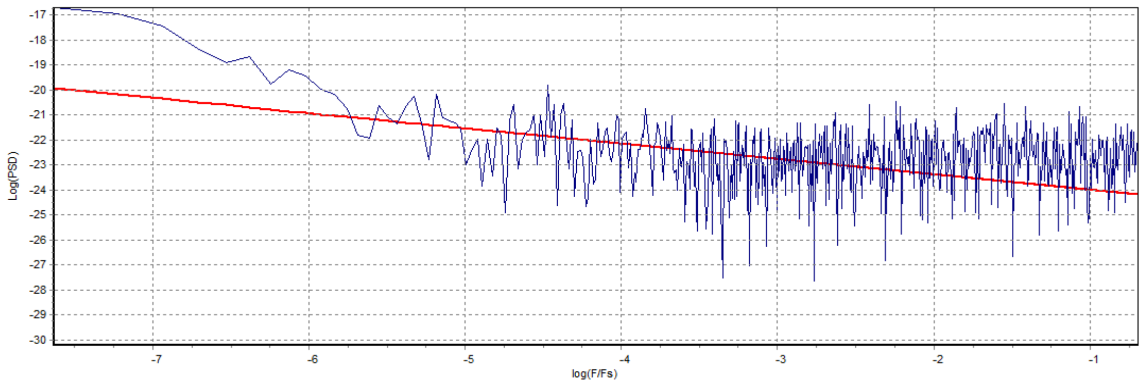

Fig. 10. MP67B Y-axis gyroscope result.

5. Conclusion

This paper characterizes successful the stochastic errors of from the output data of the IMU MP67B in Iphone6 and Iphone6Plus. The Allan variance method is an effective technique for error modeling and parameter estimation. For the MP67B, the white noise is the dominant error term for both the gyros and accelerometers. For the long cluster times, the bias instability noise appeared for the Y-axis gyro. This analysis also proves that the inertial sensor MP67B in Iphone6 and Iphone6Plus have meet requirement of a medium accuracy positioning and navigation device.

Acknowledgement

This work has been supported by Vietnam National University, Hanoi (VNU) under Project No. QG. 14. 05.

References

[1] Aggarwal P, Syed Z, Niu X, El-Sheimy, N, Standard Testing and Calibration Procedure for Low Cost MEMS Inertial Sensors and Units, The Journal of Navigation, Vol 61, 323-336, 2008.

[2] Nassar S., Accurate INS/DGPS positioning using INS data de-noising and autoregressive (AR) modeling of inertial sensor errors, Geomatica, Vol 59(3), 283-294, 2005.

[3] Paul D. Groves, Principles of GNSS, inertial, and multisensor integrated navigation systems, Artech House, 2008.

[4] Park M, Gao Y, Error and performance analysis of MEMS-based inertial sensors with a low-cost GPS receiver, Sensors,Vol 8, 2240–2261, 2008.

[5] IEEE Standard Specification Format Guide and Test Procedure for Single-Axis Interferometric Fiber Optic Gyros, IEEE Standard 952-1997(R2008), 2008.

[6] Han S, Wang J, Quantization and colored noises error modeling for inertial sensors for GPS/INS integration, IEEE Sensors Journal, Vol 11(6),1493–1502, 2011.

[7] D. W. Allan, Statistics of atomic frequency standards, Proc. IEEE, Vol. 54 (2), 221–230, 1966.

[8] Haiying Hou, Modeling inertial sensors errors using Allan variance, UCEGE reports number 20201, Master's thesis, University of Calgary, 2004.

[9] N. El-Sheimy, H. Hou and X. Niu, Analysis and Modeling of Inertial Sensors Using Allan Variance, IEEE Transations on Instrumentation and Measurement, Vol. 57(1), 140-149, 2008.

[10] Jintao Li, Jiancheng Fang, Not Fully Overlapping Allan Variance and Total Variance for Inertial Sensor Stochastic Error Analysis, IEEE Transactions On Instrumentation And Measurement, Vol 62(10), 2659-2672, 2013.

[11] Ramalingam, R., G. Anitha, and J. Shanmugam, Microelectromechnical systems inertial measurement unit error modelling and error analysis for low-cost strapdown inertial navigation system, Defence Science Journal, Vol 59(6), 2009.